Optical band gap Modification and Photodetector Properties of Au NPs Doped CuZnS Thin Films

Adel H. Omran Alkhayatt Azhar Abdul Wahab H. Ali Abdulhussein Hameed

Adilh.alkhayat@uokufa.edu.iq alallaq.g@gmail.com

University of Kufa, College of Sciences.

Abstract:

Au nanoparticles doped CuZnS (CZS) thin films were deposited by spray pyrolysis method (SPD) onto glass and silicon substrates at temperature of 330 ºC and annealed at 450ºC. Cu:Zn:S content was 1:1:2 and Au NPs dopant ratio was 4%, 6% and 8%. The structural, surface morphology, optical and photodetector properties were investigated with respect to the dopant concentration. X–Ray diffraction patterns indicate that the films have low crystallinity and polycrystalline structure nature with ZnS sphalerite cubic phase. The intensity of diffraction peaks and the crystallite size increased with the increase of Au Np's dopant ratio. The SEM images show a homogeneous and smooth uniform surface. Also AFM images reveals that the roughness increased from1.95 nm for CZS (1:1:2) to 2.64 nm for CZS:Au (4%), 4.86 nm for CZS:Au (6%) and 3.82 nm for CZS:Au (8%) thin films, these increases could be probably due to the increasing concentration of atomic gold in the CZS thin films, The average grain diameter was evaluated from the plane view images for 68.99 CZS 1:1:2 and CZS:Au NPs was (93.59–102.07 nm). Au Np's dopant ratio, the lower band gap corresponds to Cu_xS phase and double band gap confirms the alloy nature of material. The decreased in energy band gap after increasing of Au Np's dopant ratio can be attributed to the red shift of the absorption edge and to the improvement in the crystallinity, increase of Au Np's ratio leads to decrease band gap from 2.5 eV to 2.39 eV. Photodetectors CuZnS: Au Np's/Si were synthesized and I–V characteristics have been investigated, the results showed that the photocurrent increased from 0.0 to (8.65×10^{-7} A, 5.62×10^{-6} A and 5.03×10^{-6} A) at the bias voltage range of 0– 2V under illumination, and from 0.0 to (3.49×10^{-7} A, 1.9×10^{-6} A and 3.14×10^{-6}A) in the dark for CZS:Au NPs (4%, 6% and 8%) ratio, respectively. Under applied voltage of 2V, the response time was (0.8, 0.5 and 1.5 sec) respectively; whereas the recovery time was (0.6, 0.9 and 1.35 sec) and the sensitivity increased from 42.86% to 122.73%.

http://dx.doi.org/10.31257/2018/JKP/100115

Keywords: CuZnS, photodetector, Au Nano particles, Spray Pyrolysis Method, SPD.

تعديل فجوة الطاقة البصرية وخصائص الكاشف الضوئي لأغشية CuZnS المشوبة بجسيمات الذهب النانوية

عادل حبيب عمران الخياط أزهر عبدالوهاب حبيب علي عبدالحسين حميد

جامعة الكوفة/كلية العلوم

الخلاصة:

رُسبت أغشية CuZnS الرقيقة بجسيمات الذهب النانوية بطريقة الرش الكيميائي (SPD) على قواعد من الزجاج والسليكون عند درجة حرارة 330 سيليزي ولُدنت عند 450 سيليزي. كان محتوى الـ Cu:Zn:S محدد بالنسب 1:1:2 بينما نسب شائبة الذهب عند 4%، 6% و 8%. لقد تمت دراسة الخصائص التركيبية ومورفولوجية السطح مع خصائص الكاشف الضوئي نسبةً الى تركيز شائبة الذهب النانوية. أُستخلص من حيود الأشعة السينية بأن الغشاء ذات طبيعة بلورية واطئة ومتعددة التبلور بطور المكعب، وشدة نمط الحيود والحجم الحبيبي (البلوري) ازدادت بزيادة شائبة الذهب النانوية .

صور الـ SEM بينت تجانس ونعومة السطح. وأيضاً في قياسات الـ AFM حيث لوُحظَ زيادة خشونة السطح من (1.95) نانو لـ CZS 1:1:2 الى (2.64) نانو للنسبة 4%، و (4.86) نانو للنسبة 6% و (3.82) نانو للنسبة 8%. هذه الزيادة من الممكن أن تُعزى الى زيادة تركيز نسبة الشائبة لذرة الذهب في اغشية .CZS أيضاً تم حساب حجم قطر الحبيبات إعتماداً على احداثيات صور الـ AFM فوجد يتروا ح بين (93.59–102.07 نانومتر).

بوجود شائبة الذهب النانوية، حصل نقصان بفجوة الطاقة من (2.5) الى (2.39) الكترون فولط يقابل طور Cu_xS ومضاعفة فجوة الطاقة يؤكد طبيعة مكونات المادة. زيادة نسبة شائبة الذهب قادت إلى نقصان فجوة الطاقة وزحزحتها نحو الأطوال الموجية في المنطقة الحمراء من حافة الامتصاص وساهم ذلك في تحسن تبلور المادة.

أخيراً، تم تصنيع كاشف ضوئي من غشاء CuZnS:Au Np's/Si ومن ثم دراسة خصائص التيار والفولتية له، حيث وجد ان التيار الإضاءة ازداد من 0.0 الى (8.65×10^{-7} A، 5.62×10^{-6} A و 5.03×10^{-6} A)، عند تطبيق فولتية الانحياز في المدى 0 – 2 فولط تحت الاضاءة، ومن 0 الى (3.49×10^{-7} A، 1.9×10^{-6} A و 3.14×10^{-6} A) تحت الظلام لأغشية CZS:Au Np's بالنسب (4%، 6% و 8%) على التوالي. وعند تطبيق فولتية قدرها 2 فولط، وُجد ان زمن الاستجابية (0.8، 0.5 و 1.5 ثانية) على التوالي، في حين زمن الاضمحلال (0.6، 0.9 و 1.35 ثانية). وتحسسية الكاشف ازدادت من 42.86% الى 122.73%.

الكلمات المفتاحية: نحاس-خارصين-كبريت, الكواشف الضوئية، جسيمات الذهب النانوية، طريقة الرش الكيميائي.

1. Introduction

CuZnS is an alloy material having a combined structure of Cu_xS and ZnS. It is a promising absorber for solar cell and photodetectors fabrication [1], Lower bandgap films can act as good absorber while higher band gap films as good window layer for solar cells[2].

ZnS is an n-type semiconductor with a wide band gap (~3.65 eV)[4–6], and CuS is a p-type semiconductor with a band gap of (1.63-1.87 eV [3]) 2.8 eV [7] (2.52-2.58 eV [8]). It is expected that alloys of these two compounds can be either n- or p-type and will have a wide band gap. [9,10].

In addition, ZnS is a well-known semiconductor, which makes it solely absorb UV light. Absorbing only 4% of the total sunlight restricts its practical application [11]. Thus, it is highly desirable to combine ZnS semiconductor with a semiconductor with narrow band gap energy like CuS. Besides, CuS is highly susceptible to photocorrosion and it is suggested to be protected by a large band gap semiconductor [12]. Formation of pn junction using CuS (p-type) and ZnS (n-type) semiconductors increases electron hole lifetime before recombination.

CuS/ZnS has been used for photocatalytic application [13,14] and photoelectrochemical hydrogen production

[15,16]. Spray pyrolysis is a simple and inexpensive method with the capability to fabricate large area films and has been used to deposit CZS thin films. In spray pyrolysis method, the precursor solution is sprayed by a stream of a gas onto the pre-heated substrate, where upon the thermal decomposition of the precursor an adherent film forms. The most important parameters including the initial solution, the substrate surface temperature and the spray rate of solution determine the quality of the thin film [10].

In this study, the effect of Au NPs dopant concentration on the structural, optical energy gap and photodetector properties of spray deposited of CZS thin films. Also, the present work describes a chemical method for deposition of CuZnS thin films at various ratios of Au NPs. The characterization of CuZnS films was carried out by XRD and optical studies to determine their field of possible applications. The optical properties studied were; transmittance (T) and the band gap energy of the as – grown films.

2. Experimental

Copper Zinc sulphide (CuZnS) was deposited by SPD method, the solution is containing 0.1 M copper chloride dehydrate ($CuCl_2.2H_2O$), 0.1 M zinc chloride ($ZnCl_2.2H_2O$), 0.3 M thiourea $CS(NH_2)_2$, 0.01 M Chlorogoldsäure ($HAuCl_4{\cdot}xH_2O$) and distilled water in a beaker. Preparation the solution of CuZnS thin films were carried out using 20 ml glass beaker at an average room temperature of 300K. Before the deposition of the films, the substrates used were degreased in acetone for 24 hours, washed with detergent, rinsed in distilled water and dried in air. The degreased cleaned surface provide nucleation center for the growth of the films onto the substrate surface hence will result to highly adhesive and uniformly deposited films on the surface of the substrates.

The deposition solution was added and stirred to have a homogeneous mixture, and sprayed onto the substrate kept at temperature of 330 ºC. The final solution was stirred to have a homogeneous mixture.

The vacuum thermal evaporation system (Edward Auto 306) was use to deposition of Al for photoetectors by using the mask, which is usually formed by a metal (Si), as for the cleaning of silicon (Si), substrates are cleaned and degreased with ethanol and distilled water. The surface of the Si wafers is already mechanically polished to mirror like surface, Native oxides are removed by using 1:10 $HF:H_2O$ solution. Before using, the wafer was scribed by special diamond cutter then cut into small samples with appropriate sizes of about 1.5 x 1.5 cm^2. The masks are placed as closely as possible to be the substrate on which the film is to be deposited. For Photo detector measurements, it is essential to specify the form of film. For this purpose, a suitable mask is used to get the desired shape as shown in Fig.1.

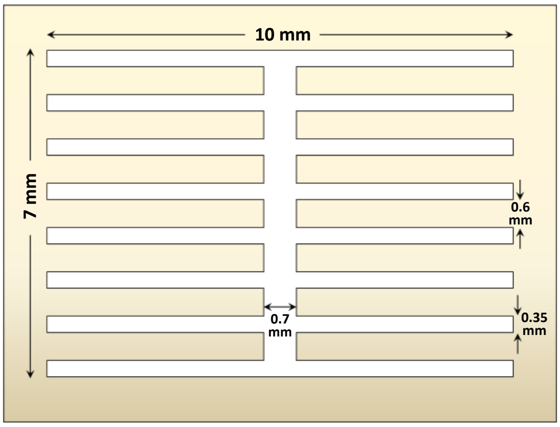

Fig.1: Grid geometry of front metal mask.

The chemical spray pyrolysis setup has been used in deposition the CuZnS:Au

NPs films on glass and Si substrates. The spray system is responsible for the spray operation, and it is achieved in periods of about 12 sec followed by ~2 mins wait, with 5 ml/hour of flow rate air. In order to deposit thin films with uniform thickness the distance between the substrate and spray nozzle was kept at 30 cm.

Then used for as metal contact deposition of **Al** on Si substrates for fabricating photodetcter. The silicon wafer (n-type) used with an (1.5-4 Ohm-cm) resistivity, thickness 508±15 and (111)-orientation.

The structural of deposited films was carried out using X-ray diffraction (XPert Pro MPD PANalytical). Cu kα radiation with wavelength 1.5406 Å, the current 30 mA, voltage 40 KV, and scanning angle varied in the range (10-70)^o.

The surface morphology of the samples is recorded by an AFM (Nanoscope III and Dimension 3100, by Veeco Instruments Inc.) and SEM (INSPECT-S50 by FEI-Netherlands-Holland) is normally carried out at 10 kV.

The optical measurements in the wavelength range (200-1100) nm using (Double Beam UV Spectrophotometer–MEGA-2100- SCINCO Company–Korea).

Keithly source meter "Model 2430 Series Source meter" tungsten lamp with power of about 70 mW at the visible incident wave length (500 nm) with 2V applied bias.

3. Result and Discussion:

Fig.2 shows the XRD patterns of pure and Au NPs doped CZS thin films with different dopant ratio (4%, 6% and 8%). The diffraction patterns indicate that the crystal structure of the prepared films has low crystallinity and polycrystalline nature. It was found that the diffraction peak of preferred orientation is along [111] plan corresponding to the sphalerite (cubic) phase appeared at 2θ = 28.46°, 28.32° and 28.41° for and Au NPs 4,6and 8% doped CuZnS thin films respectively.

These results are good agreement with the standard values of ICDD card file data (JCPDS 02-565 ZnS). When adding a low ratio of Au-dopant nanoparticle to CZS (1:1:2), from the figure it is noted that the intensity of the diffraction peaks of CuZnS films increased with the increase of Au NPs dopant ratio, therefore the doping process enhanced the crystallinity of the CZS films.

The XRD pattern a secondary peaks were appeared at 2 theta angles 23.31°, 26.71° and 47.64° related to the crystal planes (221), (100) and (220) respectively corresponding to Hexagonal CuS and Monoclinic Cu_2S phases as shown in fig. 2. These results are in good agreement with (JCPDS) card file data (26-1116 Cu_2S), (02-0820 CuS) and (33-0490 Cu_2S). Finally, all above results are in good agreement with the Literatures [4, 5, 18]

Interplanar spacing (d_{hkl}) where calculated by using Bragg's law:

$$n\lambda = 2d_{hkl}\sin\theta \quad (1)$$

and shows good agreement with the standard values as shown in table (1).

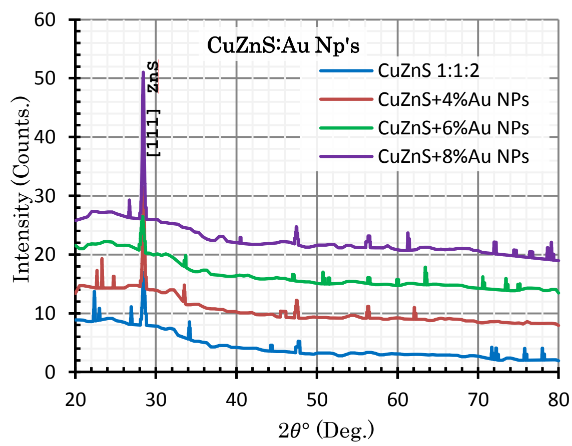

Fig.2: XRD Pattern of CZS:Au NPs thin films.

Table.1: XRD calculations for prepared thin films.

Sample	$2\theta^{o}$	***hkl***	d_{calc} Å	d_{stand} Å	a=b=c Å	FWHM	G. S. nm	$\delta\times10^{14}$ line/m^{2}
CZS 1:1:2	22.35	(004)	3.98	3.97	–	0.12	–	–
	26.94	(032)	3.31	3.29	–	0.08	–	–
	28.466	(111)	3.14	3.12	5.43863	0.31	26.027	14.747
	34.14	$(\bar{3}15)$	2.63	2.63	–	0.14	–	–
	47.64	(220)	1.91	1.90	–	0.47	–	–
CZS:Au 4%	23.31	(221)	3.82	3.76	–	0.05	–	–
	28.4601	(111)	3.13624	3.12	5.4321	0.2362	34.716	8.2974
	33.5	(114)	2.67	2.68	–	0.12	–	–
CZS:Au 6%	28.3155	(111)	3.1518	3.12	5.4321	0.3936	20.8264	23.055
	33.62	(042)	2.67	2.68	–	0.24	–	–
	63.45	(1010)	1.47	1.45	–	0.07	–	–
CZS:Au 8%	26.71	(100)	3.34	2.32	–	0.238	–	–
	28.4083	(111)	3.14184	3.12	5.44182	0.2362	34.7120	8.2993
	47.42	(110)	1.92	1.89	–	0.22	–	–
	61.29	(104)	1.51	1.49	–	0.068	–	–

After CZS thin film doped with different Au dopant concentration (4%, 6% and 8%), the SEM images [fig.3 a, b, c and d] shows a homogeneous and smooth uniform surface with no detectable micro-cracks and the morphology of the prepared films indicates that the size of the particles is increased with the increasing Au dopant concentration, that's clear in compare the Fig.3 with others. It has having perfectly spherical grains with well-defined grain boundaries and this result conforms to literature [20, 21].

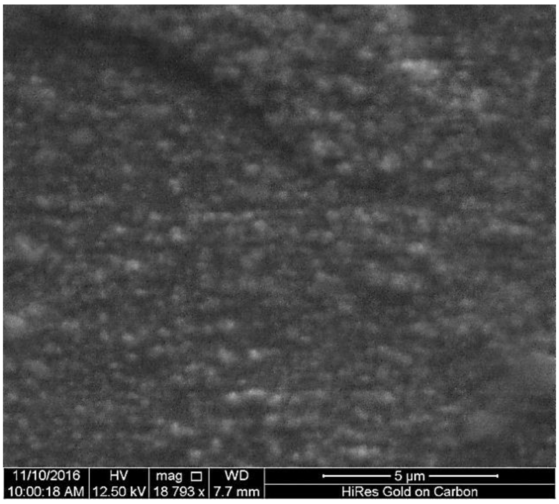

(a)

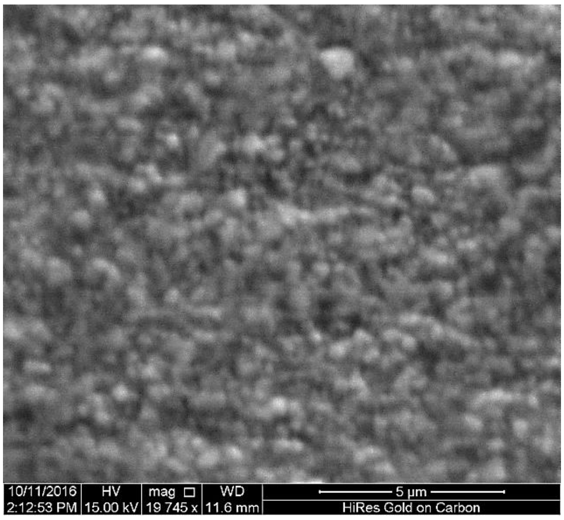

(b)

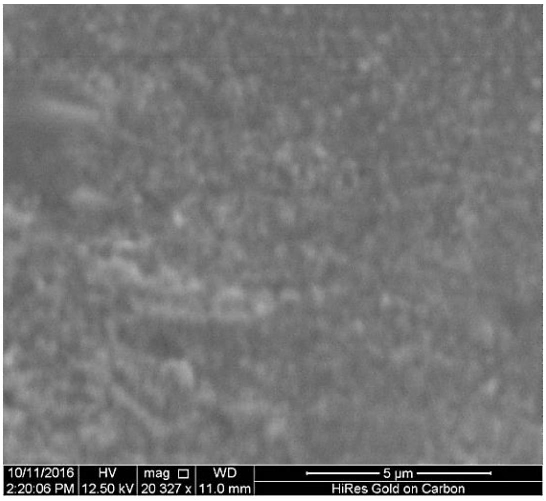

(c)

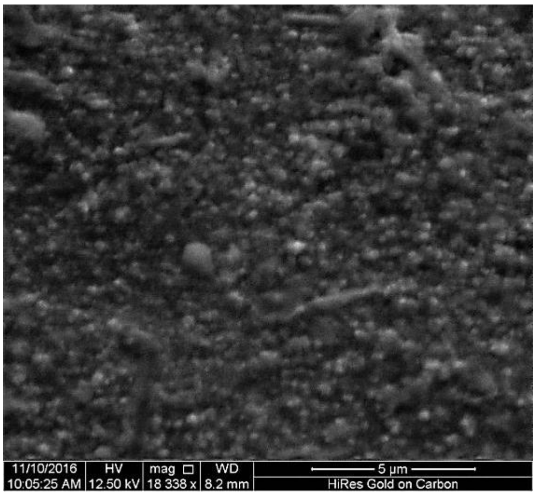

(d)

Fig.3: SEM images of a: pure, CZS doped Au NPs, b: 4%, c: 6% and d: 8% thin films.

The EDX measurements of pure CZS (1:1:2) and CZS:Au Nps thin film (4%, 6% and 8%) respectively, which can confirm the existence of elements (copper, Zinc, Sulfur and Gold) which constitute thin film structure. As shown in table (2), may be can to observed ratios of these elements and can be observed convergence in the mixing ratios of Copper, Zinc, Sulfur and Gold.

Table.2: EDX measurements of CZS:Au at ratios (4%, 6% and 8% Au NPs).

Sample	Element	norm wt %	atom at %
CZS (1:1:2) thin film	Zinc	44.88	36.32
	Copper	44.61	39.81
	Sulfur	13.50	23.88
	Total:	**100%**	**100%**
CZS:Au (4%) thin film	Copper	35.17	30.67
	Zinc	43.08	36.51
	Sulfur	18.45	31.89
	Gold	3.31	0.93
	Total:	**100%**	**100%**
CZS:Au (6%) thin film	Copper	33.92	31.40
	Zinc	47.99	43.17
	Sulfur	13.05	23.93
	Gold	5.04	1.50
	Total:	**100%**	**100%**
CZS:Au (8%) thin film	Copper	41.59	37.09
	Zinc	38.50	33.36
	Sulfur	16.11	28.46
	Gold	3.80	1.09
	Total:	**100%**	**100%**

The surface morphology of Au Nps doped CZS (1:1:2) thin films with different ratios where illustrated in the (fig.4.a, b, c, and d). it can be observe The surface texture results showed that the roughness (Sa) was increased from 2.64 nm for CZS:Au NPs (4%) to 4.86 nm for CZS:Au Nps (6%) thin films, these increases could be probably due to the increasing concentration of atomic gold Nps in the CZS thin films. The root mean square (RMS) (Sq) increased with increasing of Au NPs ratio, which is accordance with the findings of researcher [22]. The average grain diameter was evaluated from the plane view images for CZS:Au (94.51–102.07 nm) as tabulated in table (3), where the granularity accumulation distribution shown in the (fig.5 a, b, c, and d). These results were in good agreement with the XRD results. The tilted image exposes grain heights of a few tens of nanometers, as shown in table (3).

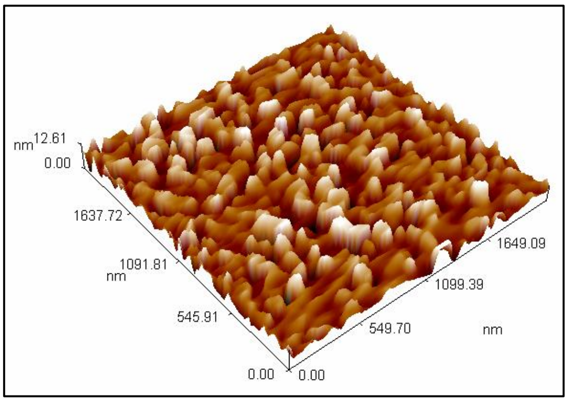

(a)

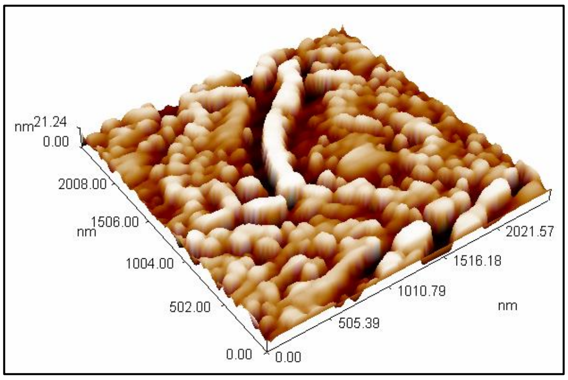

(c)

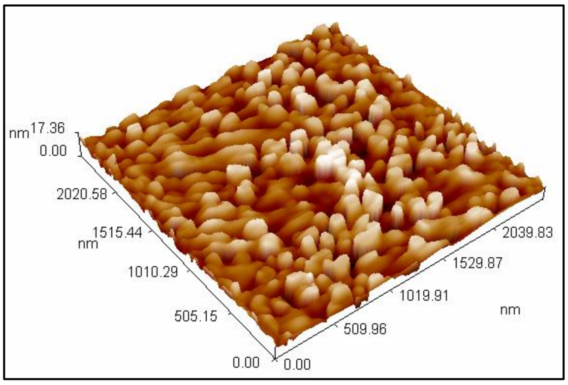

(b)

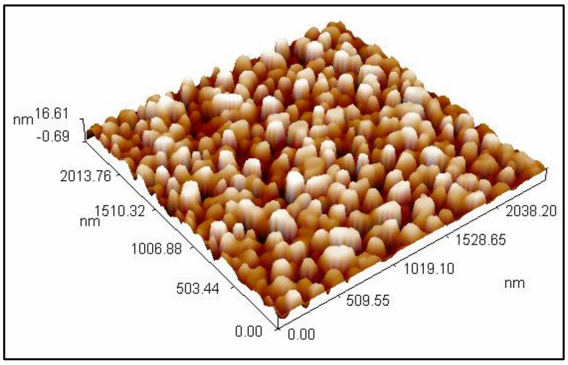

(d)

Fig.4: AFM images of a: pure, CZS doped Au NPs, b: 4%, c: 6% and d: 8% thin films.

Table.3: AFM measurements

Thin Film	Ratios of CZS	Rough ness averag e Sa (nm)	Root mean square Sq (nm)	Ten point height Sz (nm)	Average diameter (nm)
CZS: Au CZS: Au	CZS1: 1:2	1.95	2.47	12.6	68.99
	4%Au	2.64	3.3	17.3	94.51
	6%Au	4.86	5.75	12.7	102.0
	8%Au	3.82	4.55	9.69	93.59

The Granularity accumulation (accumulation) distribution charts in Fig.3 are showing the differentness before and after doping process. By increase of ratio of Au NPs, the highest average diameter is decreasing from 160 nm (for 4% Au) to 150 nm (for 6% Au) and then 130 nm (for 8% Au).

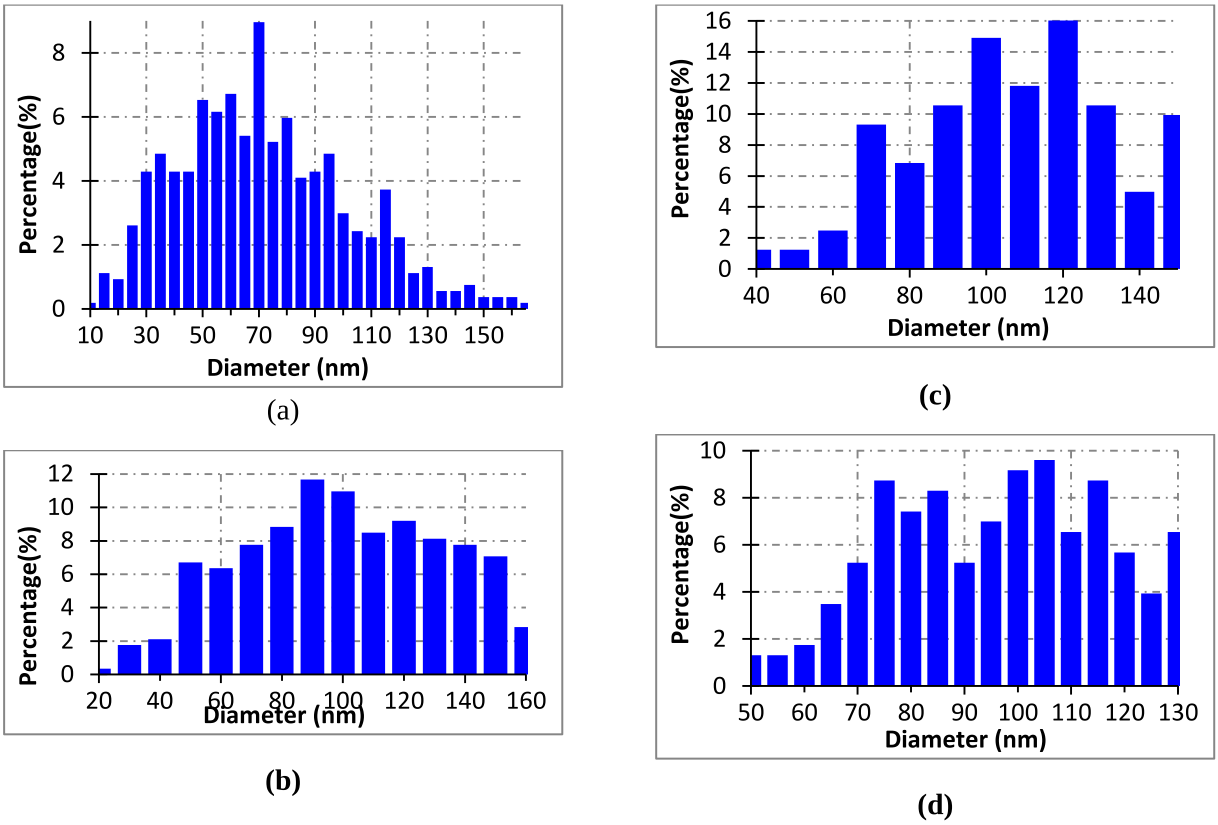

Fig.5: Granularity accumulation distribution chart for a: pure, CZS doped Au NPs, b: 4%, c: 6% and d: 8% thin films.

The optical measurement, noted that the transmittance spectrum exhibits high visible transmittance and decreases from 66% to 38% beyond the absorption edge. From the fig.6 it can be seen that the optical transmittance is influenced by increasing ratio of Au-nanoparticle.

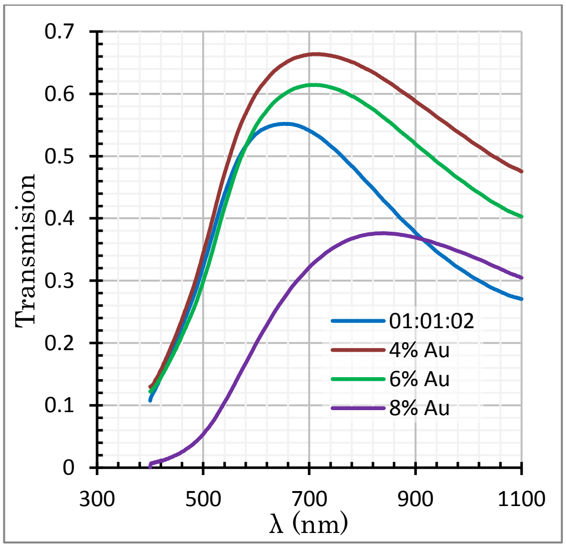

Fig.6: Optical transmittance spectra of a: pure, CZS doped Au NPs b: 4%, c: 6% and d: 8% thin films.

Figure (7) shows the value of the optical energy band gap for allowed direct transition calculated by using Tauc relation [23, 24]:

$$(\alpha h\nu) = B_x(h\nu - E_g)^r \qquad (2)$$

B_x is a constant depend on nature of material, E_g is optical energy gap, $h\nu$ is energy of absorbed photon, and r is equal (1/2 or 3/2) for direct transitions, and (2 or 3) for indirect transitions.

The energy band is estimated from the plot of $(\alpha h\nu)^2$ versus hν which is determined by extrapolating the straight line portion of the Plot to the point α = 0. The optical energy band gap of deposited CuZnS/glass thin film was found to be decreases from (2.5 to 2.39 eV) with respect to Au NPs dopant ratio. The lower band gap corresponds to Cu_xS phase and double band gap confirms the alloy nature of material. The decreased in energy band gap after increasing of of Cu/Zn content and Au NPs dopant ratio can be attributed to the red shift of the absorption edge and to the improvement in the crystallinity, where the crystallite size of the prepared films is found to increase in the range of (60-103) nm, resulting in the decrease of the band gap of the samples. These obtained optical band gaps for CuZnS thin films are consistent with those reported in the literature [25].

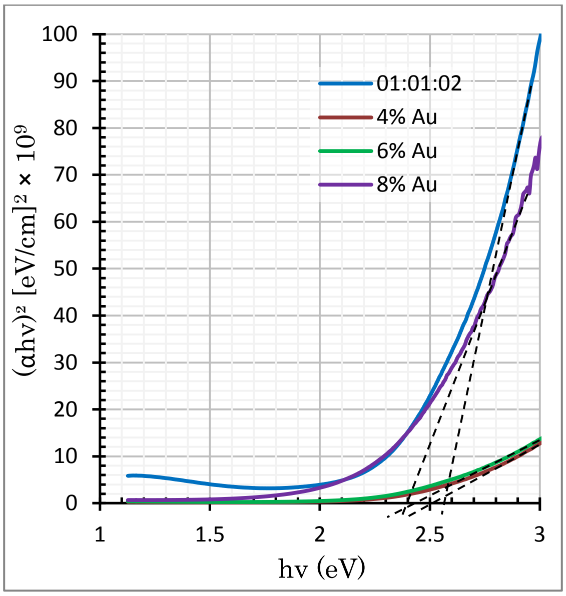

Fig.7: Variation of $(\alpha h\upsilon)^2$ vs. hυ of CZS:Au NPs thin films.

The Photodetectors measurements, it can be discuss the I–V Characteristics in state of CZS:Au/Si at (4%, 6% and 8% Au NPs) of the fabrication CZS:Au/Si photodetector with Al electrodes which is measured in under illumination (photocurrent). The photocurrent measured by using tungsten lamp with power of 70 mW/cm^2 at the visible incident wavelength with 2V applied bias voltage. It is found that the photocurrent of All samples in Fig.8 of photodetector in the forward bias because of the improvements made in the structural properties of the thin film lead to a small energy gap and therefore, the electrons need low energy to cross the energy gap consequently note that the photocurrent be higher than it was after increasing the ratios Au NPs.

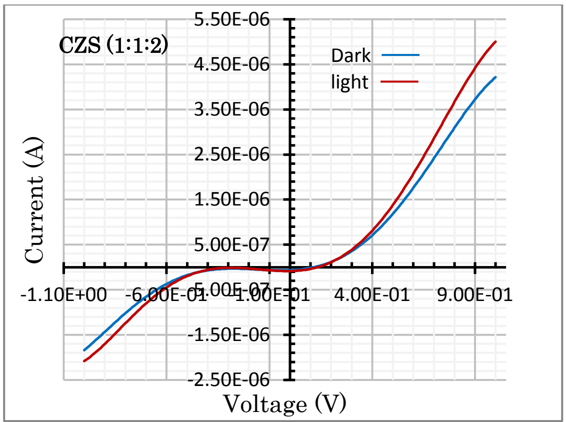

(a)

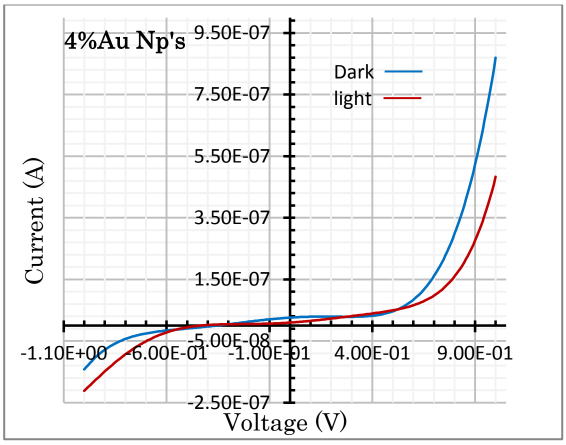

(b)

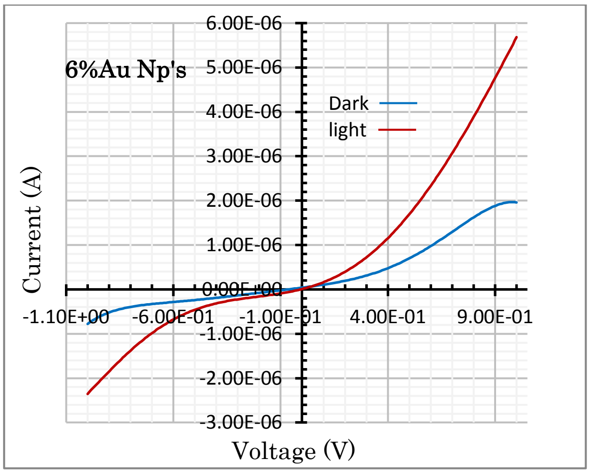

(c)

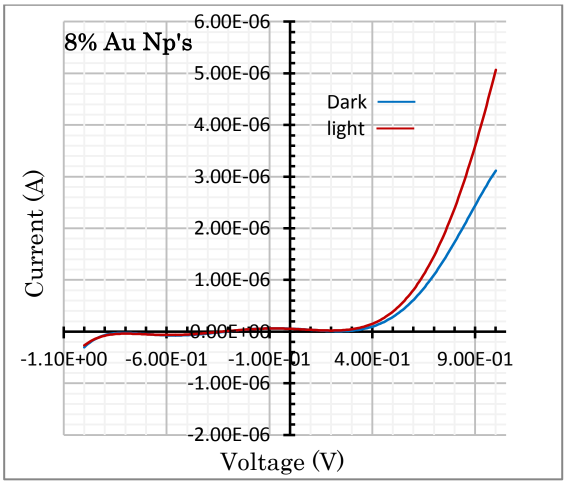

(d)

Fig.8: I-V characteristics under dark and light conditions for a: CZS/Si, CZS:Au NPs/Si , b: 4%, c: 6% and d: 8% photodetector.

Figures (9) illustrates the time dependence of the photodetector under bias voltages (2V). The device was allowed to stabilize and exposed to illumination of 500 nm chopped light with power density of 70mW/cm^2 or (7W/m^2). It can be observed that the detector has a good reproducibility.

There are some important parameters to evaluate the performance of photodetectors, these parameters are responsivity *R*, sensitivity *S*, and quantum efficiency QE [17,27];

$$R = \frac{I_{ph}}{A\, E_{opt}} \quad (3)$$

Where I_{ph} is the photocurrent, A is the illuminated area, and E_{opt} is the Light power density.

The sensitivity is given by[17,27]:

$$S(\%) = \frac{I_{light} - I_{dark}}{I_{dark}} \times 100 \quad (4)$$

Quantum efficiency is an important parameter to evaluate the performance of the device, It is given by [17,27,28]:

$$QE = \frac{hc}{q\lambda} R_{\lambda} \quad (5)$$

When a photodetector is exposed to a pulsed light source, the device exhibits a consecutive pulse current spectrum. Two important terms have been introduced in this state: The response time at 90% of the saturation current from the initial value; whereas the recovery time is 10% from it.

Photovoltaic behavior was observed at 2 V. The Energy of photons of the incident light is enough to generate an electric field which in turn produces a photocurrent. The saturation current in Figures (9) was (30, 57 and 32 μA) respectively. However, under applied voltage of 2V, the electric field produces a photocurrent that is added to the bias current. Therefore, the saturation current increased to be 57 μA.

Figures (9) shows response time is shorter than the recovery time. The response and recovery times of the device are summarized in Table 3. The response time under 2V was (0.8, 0.5 and 1.5 sec) respectively; whereas the recovery time was (0.6, 0.9 and 1.35 sec).

At comparing between ratios of Au NPs, can be noted the responsivity, sensitivity, and quantum efficiency are optimum for 6%Au NPs. These calculated by use eqs.(3, 4, and 5), and their result tabulated in Table 4.

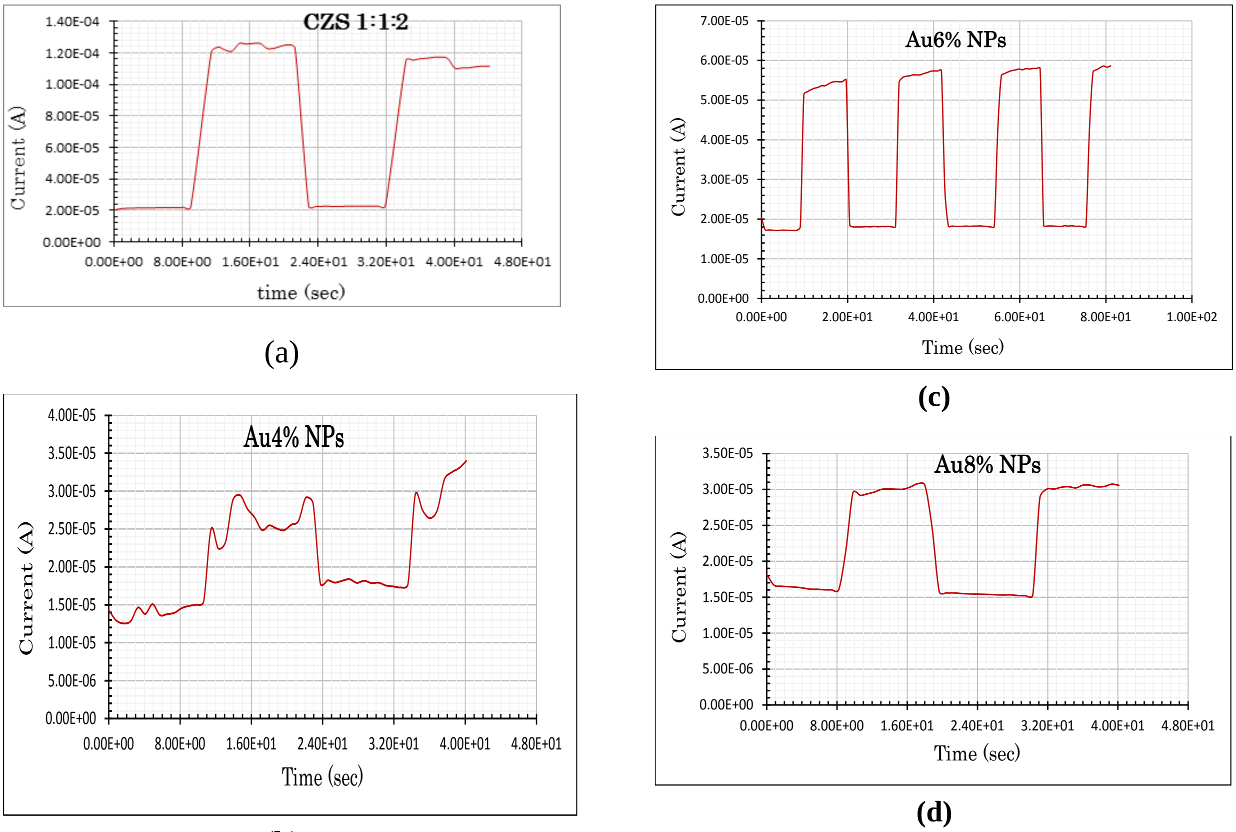

Fig.9: Photocurrent response a: CZS/Si, CZS:Au NPs/Si b: 4%, c: 6% and d: 8% photodetectors.

Table 4: Photodetecter measurements at 2V.

Sample %Au	Response Time (sec)	Recovery Time (sec)	R (A/W)	S (%)	QE (VA/W)
Pure	2.09	1.3	0.09	263.64	0.22
4%	0.8	0.6	0.01	42.86	0.02
6%	0.5	0.9	0.03	122.73	0.07
8%	1.5	1.35	0.01	52.78	0.03

4. Conclusions

From preparing Au-doped CZS thin films and CZS: Au NPs /Al/Si photodetecter by spray pyrolysis technique it can be concluded:

1. The crystalline is satisfied with a cubic (sphalerite) for ZnS preferential orientation in the (111) direction, while the CuS was crystallized in two crystallographic forms (hexagonal CuS) and (monoclinic Cu_2S). This result, show low crystalline, and then increasing of crystalline material by Au-doping. The crystallite size increased with the increasing of Au Np's ratio.
2. A uniform granular surface shows morphology of the atomic force microscope (AFM) images of thin films. The roughness average and the root mean square (RMS) are increased with the increasing of Au NPs ratio.

3. The optical properties results show that the transmittance is decreased with the increasing of Au NPs ratios in the wavelength range 600-750 nm.

4. The optical measurement shows that the pure and Au-doped CZS thin films have allowed direct energy gap (E_g) that decreased from 2.5 to 2.39 eV, the fundamental absorption edge shifted towards long wavelength and the optical energy gap decreases to low values towards the middle of the visible region which make it suitable for solar cell and photodetector applications.

5. I–V characteristics of the fabrication, CZS:Au/Si detectors with Al electrodes which is measured in the dark (dark current) under 2V applied bias voltage.

5. Reference

[1] M. S. Sreejith, et al., "Tuning of Properties of Sprayed CuZnS Films", AIP Conf. Proc. Vol. 1591, pp.1741-1743, 2014.

[2] Ezenwa I. A. and Okoli N. L., "Characterization of chemically synthesized copper zinc sulphide ($CuZnS_2$) thin films", European Open Applied Physics Journal, Vol. 1, No. 1, pp. 1-9, 2015.

[3] Saranya M, Santhosh C, Ramachandran R, Kollu P, Saravanan P, Vinoba M, et al. "Hydrothermal growth of CuS nanostructures and its photocatalytic properties", Powder Technol, 252:25e32, 2014.

[4] M.C. López, et al.,"Growth of ZnS thin films obtainedby chemical spray pyrolysis: The influence of precursors", Journal of Crystal Growth, Vol. 285, pp. 66–75, 2005.

[5] Mehdi Adelifard, et al., "Synthesis and characterization of nanostructural CuS-ZnS binary compound thin films prepared by spray pyrolysis", Optics Communications, Vol. 285, pp. 4400–4404, 2012.

[6] Mustafa Öztaş, Metin Bedir, A. Necmeddin Yazici, E. Vural Kafadar and Huseyin Toktamıs, "Characterization of copper-doped sprayed ZnS thin films", Physica B, Vol. 381, pp. 40–46, 2006.

[7] Sangamesha M, Pushpalatha K, Shekar G, Shamsundar S., "Preparation and characterization of nanocrystalline CuS thin films for dye-sensitized solar cells", ISRN Nanomater, 2013.

[8] Liu W, Ji H, Wang J, Zheng X, Lai J, Ji J, et al. "Synthesis and photo-response of CuS thin films by an in situ multideposition process at room temperature", a facile and ecofriendly approach. NANO ;10:1550032, 2015.

[9] Masaya Ichimura and Yosuke Maeda, "Conduction type of nonstoichiometric alloy semiconductor Cu_xZn_yS deposited by the photochemical deposition method", Thin Solid Films, Vol. 594, pp. 277–281, 2015.

[10] G. Heidari, et al., "Application of CuSeZnS PN junction for photoelectrochemical water splitting", International Journal of Hydrogen Energy, Vol. 42, pp. 9545–9552, 2017.

[11] Wang X, Peng W-c, Li X-y. "Photocatalytic hydrogen generation with simultaneous organic degradation by composite CdSeZnS nanoparticles under visible light", Int J Hydrogen Energy, 39:13454e61, 2014.

[12] Thuy UTD, Liem NQ, Parlett CM, Lalev GM, Wilson K, "Synthesis of CuS and CuS/ZnS core/shell nanocrystals for photocatalytic degradation of dyes under visible light", Catal Commun;44:62e7, 2014.

[13] Guan X-H, Qu P, Guan X, Wang G-S. "Hydrothermal synthesis of hierarchical CuS/ZnS nanocomposites and their photocatalytic and microwave absorption properties", RSC Adv ;4:15579e85, 2014.

[14] Yu J, Zhang J, Liu S., "Ion-exchange synthesis and enhanced visible-light photoactivity of CuS/ZnS nanocomposite hollow spheres", J Phys Chem C, 114:13642e9, 2010.

[15] Zhang J, Yu J, Zhang Y, Li Q, Gong JR. "Visible light photocatalytic H2-production activity of CuS/ZnS porous nanosheets based on photoinduced interfacial charge transfer", Nano Lett;11:4774e9, 2011.

[16] Hong Y, Zhang J, Huang F, Zhang J, Wang X, Wu Z, et al. "Enhanced visible light photocatalytic hydrogen production activity of CuS/ZnS nanoflower spheres", J Mater Chem A;3:13913e9, 2015.

[17] Saleh Hasson Abud, "Porous $In_XGa_{1-X}N$ For Sensing and Solar Cell Applications", Ph. D. thesis, Penang–Malaysia, 2014.

[18] M. Ali Yildirim, et al., "Annealing and light effect on structural, optical and electrical properties of CuS, CuZnS and ZnS thin films grown by the SILAR method", Physica E, Vol. 41, pp.1365–1372, 2009.

[19] Adnan M. M. Al- Saedi, "Study of The Effect of Doping on Structural, Optical and Electrical Properties of (ZnS) Thin Films Prepared by Chemical Spray Pyrolysis", University of Technology, Applied Sciences Department, M. Sc. Thesis, 2005.

[20] William D. Callister, Jr. "Materials Science and Engineering, an Introduction", John Wiley & Sons, Inc., the University of Utah, 2007.

[21] A.U. Ubale and V.P. Deshpande, "Effect of manganese inclusion on structural, optical and electrical properties of ZnO thin films", Journal of Alloys and Compounds, Vol. 500, pp. 138–143, 2010.

[22] Edwin Jose and M.C. Santhosh Kumar, "Room temperature deposition of highly crystalline Cu-Zn-S thin films for solar cell applications using SILAR method", Journal of Alloys and Compounds 712, 649-656, 2017.

[23] Ekbal A. Mahdi, "A Study of the Physical Properties of ZrO_2:(Co,Ti) Thin Films Prepared by Chemical Spray Pyrolysis", M. Sc. Thesis, Al-Qadisiya University, 2016.

[24] Zahraa S. AL-Akaishi, "Study of some physical properties of (PVP-PEG) polymer blends", M. Sc. Thesis, University of Kufa, 2015.

[25] Hari Singh Nalwa, "Handbook of Advanced Electronic and Photonic Materials and Devices", Vol. 8, Academic Press, 2001.

[26] M. A. Mahdi, J. J. Hassan, S. S. Ng, Z. Hassan and Naser M. Ahmed, "Synthesis and characterization of single-crystal CdS nanosheet for high-speed photodetection", Physica E, Vol. 44, pp. 1716–1721, 2012.

[27] M. A. Mahdi, J. J. Hassan, Z. Hassan and S.S. Ng, "Growth and characterization of $Zn_xCd_{1-x}S$ nanoflowers by microwave-assisted chemical bath deposition", Journal of Alloys and Compounds, Vol. 541, pp. 227–233, 2012.